

This is the accepted manuscript made available via CHORUS. The article has been published as:

Quantum time dynamics employing the Yang-Baxter equation for circuit compression

Bo Peng, Sahil Gulania, Yuri Alexeev, and Niranjana Govind

Phys. Rev. A **106**, 012412 — Published 8 July 2022

DOI: [10.1103/PhysRevA.106.012412](https://doi.org/10.1103/PhysRevA.106.012412)

Quantum time dynamics employing the Yang-Baxter equation for circuit compression

Bo Peng*

*Physical and Computational Sciences Directorate,
Pacific Northwest National Laboratory, Richland, Washington 99352, United States*

Sahil Gulania[†]

Mathematics and Computer Science Division, Argonne National Laboratory, Lemont, Illinois 60439, United States

Yuri Alexeev[‡]

Computational Science Division, Argonne National Laboratory, Lemont, Illinois 60439, United States

Niranjan Govind[§]

*Physical and Computational Sciences Directorate,
Pacific Northwest National Laboratory, Richland, Washington 99352, United States*

(Dated: June 21, 2022)

Quantum time dynamics (QTD) is considered a promising problem for quantum supremacy on near-term quantum computers. However, QTD quantum circuits grow with increasing time simulations. This study focuses on simulating the time dynamics of 1D integrable spin chains with nearest neighbor interactions. We have proved the existence of a reflection symmetry in the quantum circuit employed for simulating the time evolution of certain classes of 1D Heisenberg model Hamiltonians by virtue of the quantum Yang-Baxter equation, and how this symmetry can be exploited to compress and produce a shallow quantum circuit. With this compression scheme, the depth of the quantum circuit becomes independent of step size and only depends on the number of spins. We show that the depth of the compressed circuit is rigorously a linear function of the system size for the studied Heisenberg model Hamiltonians in the present work. As a consequence, the number of CNOT gates in the compressed circuit only scales quadratically with the system size, which allows for the simulations of time dynamics of very large 1D spin chains. We derive the compressed circuit representations for different special cases of the Heisenberg Hamiltonian. We compare and demonstrate the effectiveness of this approach by performing simulations on quantum computers.

I. INTRODUCTION

Simulation of statistical mechanical models is a vital application for classical and quantum computing [1]. It is also well known that the partition function of a $d + 1$ -dimensional classical system can be mapped to the partition function of a d -dimensional quantum system [2–4]. This deep classical to quantum connection can give insights into quantum universality classes using appropriate classical counterparts. It might allow one to use these effective models to study critical points and phase transitions of magnetic systems, where the spins of the magnetic systems are treated quantum mechanically.

Quantum Ising and Heisenberg models [5] represent some of the simplest models that can describe the behavior of magnetic systems. However, 2D- and 3D-quantum lattice simulations remain challenging for classical computing. A possible solution is to use quantum computing, given that it is only natural to simulate quantum systems with quantum computers, as suggested by Benioff [6] and Feynman [7]. The idea of using quantum computing on

quantum devices is compelling since it paves the way for systematic improvements of quantum technologies. The exploration of this approach is at the core of several research efforts in quantum information sciences [8]. In particular, the development of new generations of quantum models and associated simulations on existing and upcoming noisy intermediate-scale quantum (NISQ) [9] devices is of special interest.

Quantum integrable systems [5, 10] typically refer to systems where the dynamics are two-body reducible. Put another way, even though the Hilbert space increases exponentially with increasing system size in these systems, the two-body reducibility, in combination with the algebraic Bethe ansatz [5, 11, 12], can be used to obtain explicit solutions, under certain conditions, by solving a set of nonlinear equations that scales only linearly with system size. The quantum Yang-Baxter equation (YBE) or star-triangle relation [10, 13–15] is a consequence of this factorization. The algebraic formulation of quantum integrable systems makes them ideal tools to study a broad range of low-dimension physical models. Historically, the isotropic interacting quantum spin chain, or Heisenberg model [16], was the first quantum integrable system, whose exact eigenstates were obtained through the Bethe ansatz approach as a superposition of plane waves [11, 17–21]. Other quantum integrable models include the Lieb-Liniger model [22, 23], Hubbard

* peng398@pnnl.gov

† sgulania@anl.gov

‡ yuri@anl.gov

§ niri.govind@pnnl.gov

model [24], Calogero–Sutherland model [5, 25–29], models from quantum field theory such as the sine-Gordon model [30, 31], and several subclasses of the Heisenberg model (e.g., XXZ model) [16, 32].

An important open question in quantum integrable systems is time evolution, or the response dynamics where the system responds to a change of parameters. This problem requires sufficiently accurate control of the time evolution of the system, which is governed by the time-dependent Schrödinger or Dirac equation of the quantum state in the Hilbert space. The time evolution problem is also closely related to the computation of the asymptotic state of quantum integrable models, or in a more general sense the thermalization and ergodic/nonergodic behaviors of these models. Several conjectures have been proposed in this context [33–35]. For example, in the Heisenberg spin chain, quantum quenches of the XXZ model have been studied by embedding the generalized Gibbs ensemble hypothesis into the quantum transfer matrix framework [36, 37]. Nevertheless, these studies are still far from conclusive. Other types of quantum integrability are known in explicitly time-dependent quantum problems, such as the driven Tavis–Cummings model [38, 39].

Quantum circuits representing quantum time dynamics (QTD) are well known to grow with increasing time simulations. In the present era of noisy quantum computers, circuits must be as shallow as possible for meaningful results. With this as the overarching theme, we focus on QTD of 1D integrable spin chains with nearest-neighbor interactions. In particular, noticing the difference between the integrability using Bethe ansatz and the integrability via mapping to free fermions, as a preliminary step our present work is only focused on circuit compression technique for accurately and efficiently simulating the time dynamics of free fermions on noisy quantum device. We show how the quantum YBE can be used to compress and produce a shallow quantum circuit, where the depth becomes independent of step size and depends only on the number of spins. The depth of the compressed circuit is rigorously a linear function of the system size for the studied Heisenberg model Hamiltonians in the present work. As a consequence, the number of CNOT gates in the compressed circuit only scales quadratically with the system size. This allows for simulations of time dynamics of very large 1D spin chains. Compressed circuit representations are derived for different special cases of the Heisenberg Hamiltonian.

As a proof of principle, we demonstrate the effectiveness of this approach by performing simulations of the Heisenberg XY model (or XY model, in brief) on quantum devices. The time evolution of the XY model is an active area of research and has been approached from many directions. Verstraete and co-workers [40] utilized the quantum Fourier transform with the Bogoliubov transformation to perform time dynamics efficiently on a quantum computer. Besides, we note that there are also several other approaches reported recently for compress-

ing quantum circuits for dynamics using both integrable and non-integrable models [41–45]. For example, in a similar study to this work, Bassman and co-workers [46–48] reported simulations of the XY model by conjecturing the relationship between the reflection symmetry and YBE-like “turn over” operation and provided numerical evidence for the transformation. However, no connection to the YBE was made. Here, we not only recognize the connection, but also rigorously derive the analytical expressions and compressed circuit representations for different special cases of the Heisenberg Hamiltonian. This connects our work to the broader and deeper context of the YBE duality and integrable quantum computation. For the rest of this paper we will tacitly assume the quantum YBE and omit quantum for brevity.

II. THEORY

For completeness, we start by reviewing relevant background material, with a brief introduction to the Heisenberg Hamiltonian, quantum time dynamics, and the Yang–Baxter equation.

A. Heisenberg Hamiltonian

The Heisenberg Hamiltonian [49–51] is widely used to study magnetic systems, where the magnetic spins are treated quantum mechanically. The Hamiltonian, including only spin-spin interactions, can be written as

$$\hat{H} = - \sum_{\alpha} \{ J_{\alpha} \sum_{i=1}^{N-1} \sigma_i^{\alpha} \otimes \sigma_{i+1}^{\alpha} \}, \quad (1)$$

where α sums over $\{x, y, z\}$, the coupling parameter J_{α} denotes the exchange interaction between nearest-neighbour spins along the α -direction, and σ_i^{α} is the α -Pauli operator on the i th spin. Interaction with the magnetic field can be included in this Hamiltonian as

$$\hat{H}_{in}(t) = \hat{H} - h_{\beta}(t) \sum_{i=1}^N \sigma_i^{\beta}, \quad (2)$$

where $h_{\beta}(t)$ is the time amplitude of the external magnetic field along the $\beta \in \{x, y, z\}$ direction. Several variations of this model are known in the literature, which are categorized depending on the relation between J_x , J_y , and J_z . This Heisenberg Hamiltonian represents quantities based on the electronic structure of the system, where the Coulomb interaction and hopping are mapped onto spin variables [52, 53]. A simple variant of the Heisenberg model is the 1D XY model that was first introduced and solved by Lieb, Schultz, and Mattis [54] in the absence of a magnetic field and later by Katsura [55, 56] and Niemeijer [57] in a finite external field. The XY model describes a 1D lattice with spin variables labeling every lattice point. The spins are limited to interact only with their nearest neighbors in an anisotropic way.

B. Time Evolution

Quantum state evolution [58, 59] is governed by the Schrödinger or Dirac equation

$$i\hbar \frac{\partial}{\partial t} |\psi(t)\rangle = \hat{H} |\psi(t)\rangle. \quad (3)$$

The solution to this equation can be expressed as

$$|\psi(t)\rangle = e^{-i\hat{H}t/\hbar} |\psi(0)\rangle, \quad (4)$$

where $e^{-i\hat{H}t/\hbar}$ is the evolution operator. In the 1D Heisenberg model, with the exception of $N = 2$, all the elements in the Hamiltonian do not commute with each other, and hence the exponential of \hat{H} cannot be written as a product of exponentials. For $N = 2$,

$$e^{-i\hat{H}t/\hbar} = \prod_{\alpha} e^{iJ_{\alpha}t(\sigma_1^{\alpha} \otimes \sigma_2^{\alpha})/\hbar}, \quad (5)$$

where each term is straightforward to evaluate, as shown below.

$$e^{iJ_x t(\sigma_1^x \otimes \sigma_2^x)/\hbar} = \begin{pmatrix} \cos(\theta_x) & 0 & 0 & i \sin(\theta_x) \\ 0 & \cos(\theta_x) & i \sin(\theta_x) & 0 \\ 0 & i \sin(\theta_x) & \cos(\theta_x) & 0 \\ i \sin(\theta_x) & 0 & 0 & \cos(\theta_x) \end{pmatrix}$$

$$e^{iJ_y t(\sigma_1^y \otimes \sigma_2^y)/\hbar} = \begin{pmatrix} \cos(\theta_y) & 0 & 0 & -i \sin(\theta_y) \\ 0 & \cos(\theta_y) & i \sin(\theta_y) & 0 \\ 0 & i \sin(\theta_y) & \cos(\theta_y) & 0 \\ -i \sin(\theta_y) & 0 & 0 & \cos(\theta_y) \end{pmatrix}$$

$$e^{iJ_z t(\sigma_1^z \otimes \sigma_2^z)/\hbar} = \begin{pmatrix} e^{i\theta_z} & 0 & 0 & 0 \\ 0 & e^{-i\theta_z} & 0 & 0 \\ 0 & 0 & e^{-i\theta_z} & 0 \\ 0 & 0 & 0 & e^{i\theta_z} \end{pmatrix} \quad (6)$$

Here, $\theta_{\alpha} = tJ_{\alpha}/\hbar$. For $N = 3$, some terms do not commute. For instance, if p_{12} represents the Heisenberg interaction (Eq. (5)) between spins 1 and 2 and p_{23} represents interaction between spins 2 and 3, then p_{12} does not commute with p_{23} . As a result, one cannot decompose the time evolution operator as a product of two-body evolution operators. The Trotter decomposition can be used to rewrite the time evolution operator in terms of two-body components as follows:

$$e^{-i\hat{H}t/\hbar} = \left[\left(\prod_{\alpha} e^{i\theta_{\alpha}(\sigma_1^{\alpha} \otimes \sigma_2^{\alpha} \otimes \mathbb{I})/n} \right) \times \left(\prod_{\alpha} e^{i\theta_{\alpha}(\mathbb{I} \otimes \sigma_2^{\alpha} \otimes \sigma_3^{\alpha})/n} \right) \right]^n + \mathcal{O}(t/n), \quad (7)$$

where the error scales linearly with the time step, namely, t/n , which can be a significant source of error. This can be mitigated by taking a smaller step size. However, this results in an overall increase in the computation cost. As

analyzed in Refs. 60, 61, for the Heisenberg model Hamiltonian, the gate complexity associated with the quantum simulation employing product formulas scales as $\mathcal{O}(t^2/\epsilon)$ and $\mathcal{O}(5^{2k}t^{1+1/2k}/\epsilon^{1/2k})$ for 1st order and $2k$ -th order, respectively, with t representing the simulation time and ϵ the allowed error. The desired upper bounds, including analytic, minimized, and empirical bounds, on the allowed error ϵ has been extensively explored and discussed previously (see Refs. 60–64) for choosing a reasonable n -segment such that the asymptotic complexity of the production formula algorithm can be improved. In a more general sense, one can also explore other routes to balance accuracy and computation cost. For example, extending the evolution operator to systems with $N > 3$, one can observe two major commuting families as shown in Fig.1. All elements in the orange family commute, and all elements in the blue family commute. Therefore the evolution operator can be written as a product of exponentials within the families without Trotter decomposition.



FIG. 1. 1D spin chain showing two families (orange and blue) in which all elements in each family commute within that family.

C. Yang–Baxter Equation

The Yang–Baxter equation was introduced independently in theoretical physics by Yang [13] in the late 1960s and by Baxter [65] in statistical mechanics in the early 1970s. This relation has also received much attention in many areas of theoretical physics, classification of knots, scattering of subatomic particles, nuclear magnetic resonance, and ultracold atoms and, more recently, in quantum information science [66–71].

The YBE connection to quantum computing originates from investigating the relationship between topological entanglement, quantum entanglement, and quantum computational universality. Of particular interest is how the global topological relationship in spaces (e.g., knotting and linking) corresponds to the entangled quantum states and how the CNOT gate, for instance, can in turn be replaced by another unitary gate R to maintain universality. It turns out these unitary R gates, which serve to maintain the universality of quantum computation and also serve as solutions for the condition of topological braiding, are unitary solutions to the YBEs [14]. Briefly, the relation is a consistency or exchange condition that allows one to factorize the interactions of three bodies into a sequence of pairwise interactions under certain conditions. Formally, this can be written as

$$(\mathcal{R} \otimes \mathbb{I})(\mathbb{I} \otimes \mathcal{R})(\mathcal{R} \otimes \mathbb{I}) = (\mathbb{I} \otimes \mathcal{R})(\mathcal{R} \otimes \mathbb{I})(\mathbb{I} \otimes \mathcal{R}), \quad (8)$$

where the \mathcal{R} operator is a linear mapping $\mathcal{R} : V \otimes V \rightarrow$

$V \otimes V$ defined as a twofold tensor product generalizing the permutation of vector space V . In circuit language, \mathcal{R} represents a parametrized unitary gate. In particular, although there exists \mathcal{R} gate structures of higher dimension [72], we limit our discussion of \mathcal{R} in the present context as a two-qubit gate parametrized by a phase factor and a rotation (see e.g. Eq. (12)). This relation also yields a sufficiency condition for quantum integrability in 1D quantum systems and provides a systematic approach to construct integrable models. Since a detailed discussion of this topic is beyond the scope of this paper, we refer the reader to more comprehensive works and reviews on the subject [10, 14].

III. CIRCUIT REPRESENTATION OF THE TIME EVOLUTION OPERATOR

Since the evolution operator is a unitary matrix, there exists a quantum circuit that can perform this operation efficiently on a quantum computer. First, we will find the quantum circuit for two spins and later extend it to N spins with nearest-neighbor interactions in 1D. Each spin can be mapped to a qubit, and the evolution of the spin system can be mapped to a quantum circuit. Using Eqs. (5) and (6), we have

$$\prod_{\alpha=x,y,z} e^{iJ_{\alpha}t(\sigma_1^{\alpha} \otimes \sigma_2^{\alpha})/\hbar} = \begin{pmatrix} e^{i\theta_z} \cos(\gamma) & 0 & 0 & ie^{i\theta_z} \sin(\gamma) \\ 0 & e^{-i\theta_z} \cos(\delta) & ie^{-i\theta_z} \sin(\delta) & 0 \\ 0 & ie^{-i\theta_z} \sin(\delta) & e^{-i\theta_z} \cos(\delta) & 0 \\ ie^{i\theta_z} \sin(\gamma) & 0 & 0 & e^{i\theta_z} \cos(\gamma) \end{pmatrix} \quad (9)$$

where $\gamma = \theta_x - \theta_y$ and $\delta = \theta_x + \theta_y$. The optimal circuit for this matrix is

$$\prod_{\alpha} e^{iJ_{\alpha}t(\sigma_1^{\alpha} \otimes \sigma_2^{\alpha})/\hbar} = \begin{array}{c} \text{---} \bullet \text{---} \boxed{R_x(2\theta_x)} \text{---} \boxed{H} \text{---} \bullet \text{---} \boxed{S} \text{---} \boxed{H} \text{---} \bullet \text{---} \boxed{R_x(-\pi/2)} \text{---} \\ \oplus \text{---} \boxed{R_z(-2\theta_z)} \text{---} \oplus \text{---} \boxed{R_z(-2\theta_y)} \text{---} \oplus \text{---} \boxed{R_x(\pi/2)} \text{---} \end{array} \quad (10)$$

The evolution operator for any time step can be represented by using this circuit. In addition, it is also a constant depth circuit for each time step since the number of one- and two-qubit gates does not increase with the time step. The quantum circuit for a spin chain with more than two spins in 1D can be derived by using Eq. (10) and the Trotter decomposition.

Two commuting families of operators exist, as shown in Fig. 2, as orange and blue two-qubit gates, respectively. The accuracy of the simulation for a given time depends on the Trotter step (t/n). As a consequence of Trotterization, the quantum circuit for time evolution grows linearly with the time step. Figure 2 shows the quantum circuit for a given time t using n Trotter steps. Each Trotter step is composed of a bilayer of two-qubit gates. The first layer acts on the first two qubits, followed by the third and then the fourth qubits and so on. Orange

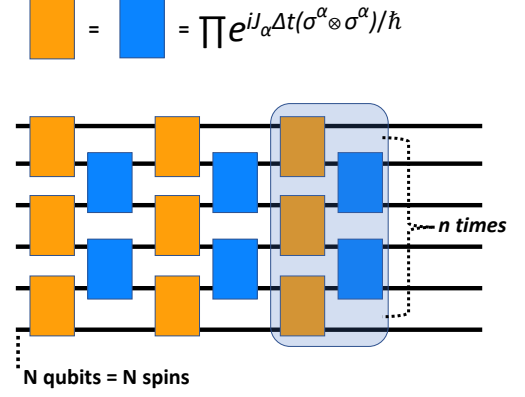


FIG. 2. Quantum circuit for time evolution of N spins, composed of n alternative layers using the Trotter approximation.

rectangles in Fig. 2 represent the first layer. The second layer of two-qubit gates starts from the second qubit and acts on the next two qubits. Blue rectangles in Fig. 2 represent the second layer. Both orange and blue rectangles combine to form an *alternative layer*, covering all possible nearest-neighbor interactions.

IV. CIRCUIT COMPRESSION USING THE YANG-BAXTER EQUATION

In Section III we showed the generalized circuit for time evolution of N spins in 1D. In this section we will utilize the YBE to simplify the generalized quantum circuit for arbitrary time steps. First, we will show the existence of a unique reflection symmetry for a quantum circuit composed of alternative layers. Next, we will show the merge identity for two-qubit gates. We will also show how reflection symmetry combined with the merge identity allows for the compression of a quantum circuit of any length to a finite depth.

A. Reflection Symmetry and Merge Identity

The evolution operator for the Heisenberg Hamiltonian on two qubits is given by Eq. (9). When there are two evolution operators with different parameters on the same two qubits, they can be merged and represented via a single operator as shown below:

$$\mathcal{R}^{ij}(\theta_x^1, \theta_y^1, \theta_z^1) \cdot \mathcal{R}^{ij}(\theta_x^2, \theta_y^2, \theta_z^2) = \mathcal{R}^{ij}(\theta_x^1 + \theta_x^2, \theta_y^1 + \theta_y^2, \theta_z^1 + \theta_z^2). \quad (11)$$

In the rest of this article we will call Eq. (11) the merge identity. Diagrammatic representation of the YBE is shown in the top panel of Fig. 6, where \mathcal{R}^{ij} represents the operator acting on i, j qubits. By using this symmetry repeatedly, one can prove the existence of reflection symmetry in n qubits composed of $n/2$ alternative layers (see the proof in Appendix A). The bottom panel

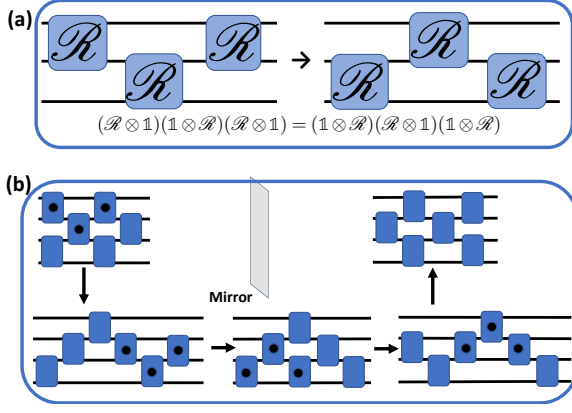


FIG. 3. (a) Quantum circuit representation of the YBE for three qubits. (b) Reflection symmetry is achieved by using the YBE four times on four qubits (action of YBE on which triplets is shown by black dots).

of Fig. 6 shows how reflection symmetry is achieved for four qubits using the YBE three times.

Reflection symmetry combined with the merge identity allows for the compression of N alternative layers of gates to $N/2$ alternative layers for N qubits. Figure 4 shows the use of reflection symmetry combined with the merge identity for four qubits. A third alternative layer can be merged into the previous two layers. Therefore, any number of alternative layers can be compressed into two alternative layers.

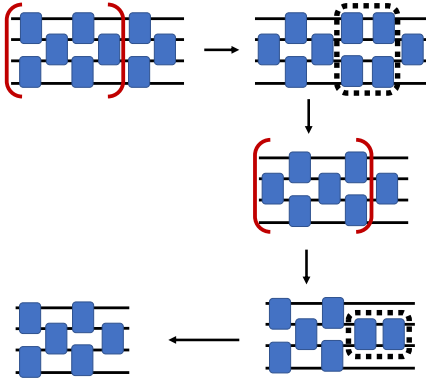


FIG. 4. Compression scheme for 4 qubits. Reflection symmetry exists with two layers of alternative gates. Addition of a third layer can be absorbed into the two layers by recursive usage of reflection symmetry (red bracket) via the YBE and merge identity (black dotted box).

B. Algebraic Condition for Reflection Symmetry

In the preceding section we showed that reflection symmetry is a sufficient condition for performing circuit compression. An interesting follow-up question is “How

would one know whether reflection symmetry can be applied to a quantum dynamics simulation of a given Hamiltonian?” To answer this question, one needs to show whether algebraic relations of phases and rotations exist before and after the reflection. Given a general time propagator such as (9), however, an exhaustive search and rigorous proof appear challenging. Because of the lack of rigorous algebraic relations, YBE-like relations can only be conjectured, as shown in previous work (see, for example, 46), thus making the compression of the circuit a heuristic process. In this section we show that some algebraic relations can be obtained rigorously for at least a few special cases of (9). In particular, we propose the following theorem.

Theorem I Given the time evolution operator that takes the following form,

$$\mathcal{R}(\gamma, \delta) = \begin{pmatrix} e^{i\delta} \cos(\gamma) & 0 & 0 & ie^{i\delta} \sin(\gamma) \\ 0 & e^{-i\delta} \cos \gamma & ie^{-i\delta} \sin \gamma & 0 \\ 0 & ie^{-i\delta} \sin \gamma & e^{-i\delta} \cos \gamma & 0 \\ ie^{i\delta} \sin(\gamma) & 0 & 0 & e^{i\delta} \cos(\gamma) \end{pmatrix}, \quad (12)$$

the following YBE holds

$$(\mathcal{R}(\gamma_1, \delta_1) \otimes \mathbb{I})(\mathbb{I} \otimes \mathcal{R}(\gamma_2, \delta_2))(\mathcal{R}(\gamma_3, \delta_3) \otimes \mathbb{I}) \\ = (\mathbb{I} \otimes \mathcal{R}(\gamma_4, \delta_4))(\mathcal{R}(\gamma_5, \delta_5) \otimes \mathbb{I})(\mathbb{I} \otimes \mathcal{R}(\gamma_6, \delta_6)) \quad (13)$$

if and only if the following 16 relations between the γ 's and δ 's are satisfied:

$$s_{\gamma_2} c_{\gamma_1 - \gamma_3} c_{\delta_1 - \delta_3} s_{\delta_2} = c_{\gamma_5} s_{\gamma_4 + \gamma_6} s_{\delta_4 + \delta_6} c_{\delta_5} \quad (14)$$

$$c_{\gamma_2} c_{\gamma_1 - \gamma_3} c_{\delta_1 + \delta_3} s_{\delta_2} = c_{\gamma_5} c_{\gamma_4 + \gamma_6} s_{\delta_4 + \delta_6} c_{\delta_5}, \quad (15)$$

$$-s_{\gamma_2} c_{\gamma_1 + \gamma_3} s_{\delta_1 - \delta_3} c_{\delta_2} = c_{\gamma_5} s_{\gamma_4 - \gamma_6} c_{\delta_4 + \delta_6} s_{\delta_5}, \quad (16)$$

$$c_{\gamma_2} c_{\gamma_1 + \gamma_3} s_{\delta_1 + \delta_3} c_{\delta_2} = c_{\gamma_5} c_{\gamma_4 - \gamma_6} c_{\delta_4 + \delta_6} s_{\delta_5}, \quad (17)$$

$$s_{\gamma_2} c_{\gamma_1 + \gamma_3} c_{\delta_1 - \delta_3} c_{\delta_2} = c_{\gamma_5} s_{\gamma_4 + \gamma_6} c_{\delta_4 + \delta_6} c_{\delta_5}, \quad (18)$$

$$c_{\gamma_2} c_{\gamma_1 + \gamma_3} c_{\delta_1 + \delta_3} c_{\delta_2} = c_{\gamma_5} c_{\gamma_4 + \gamma_6} c_{\delta_4 + \delta_6} c_{\delta_5}, \quad (19)$$

$$-s_{\gamma_2} c_{\gamma_1 - \gamma_3} s_{\delta_1 - \delta_3} s_{\delta_2} = c_{\gamma_5} s_{\gamma_4 - \gamma_6} s_{\delta_4 + \delta_6} s_{\delta_5}, \quad (20)$$

$$c_{\gamma_2} c_{\gamma_1 - \gamma_3} s_{\delta_1 + \delta_3} s_{\delta_2} = c_{\gamma_5} c_{\gamma_4 - \gamma_6} s_{\delta_4 + \delta_6} s_{\delta_5}, \quad (21)$$

$$s_{\gamma_2} s_{\gamma_1 + \gamma_3} c_{\delta_1 - \delta_3} c_{\delta_2} = s_{\gamma_5} s_{\gamma_4 + \gamma_6} c_{\delta_4 - \delta_6} c_{\delta_5}, \quad (22)$$

$$c_{\gamma_2} s_{\gamma_1 + \gamma_3} c_{\delta_1 + \delta_3} c_{\delta_2} = s_{\gamma_5} c_{\gamma_4 + \gamma_6} c_{\delta_4 - \delta_6} c_{\delta_5}, \quad (23)$$

$$s_{\gamma_2} s_{\gamma_1 - \gamma_3} s_{\delta_1 - \delta_3} s_{\delta_2} = s_{\gamma_5} s_{\gamma_4 - \gamma_6} s_{\delta_4 - \delta_6} s_{\delta_5}, \quad (24)$$

$$-c_{\gamma_2} s_{\gamma_1 - \gamma_3} s_{\delta_1 + \delta_3} s_{\delta_2} = s_{\gamma_5} c_{\gamma_4 - \gamma_6} s_{\delta_4 - \delta_6} s_{\delta_5}, \quad (25)$$

$$-s_{\gamma_2} s_{\gamma_1 - \gamma_3} c_{\delta_1 - \delta_3} s_{\delta_2} = s_{\gamma_5} s_{\gamma_4 + \gamma_6} s_{\delta_4 - \delta_6} c_{\delta_5}, \quad (26)$$

$$-c_{\gamma_2} s_{\gamma_1 - \gamma_3} c_{\delta_1 + \delta_3} s_{\delta_2} = s_{\gamma_5} c_{\gamma_4 + \gamma_6} s_{\delta_4 - \delta_6} c_{\delta_5}, \quad (27)$$

$$-s_{\gamma_2} s_{\gamma_1 + \gamma_3} s_{\delta_1 - \delta_3} c_{\delta_2} = s_{\gamma_5} s_{\gamma_4 - \gamma_6} c_{\delta_4 - \delta_6} s_{\delta_5}, \quad (28)$$

$$c_{\gamma_2} s_{\gamma_1 + \gamma_3} s_{\delta_1 + \delta_3} c_{\delta_2} = s_{\gamma_5} c_{\gamma_4 - \gamma_6} c_{\delta_4 - \delta_6} s_{\delta_5}, \quad (29)$$

where s_p and c_p denote $\sin(p/2)$ and $\cos(p/2)$, respectively.

The proof of **Theorem I** is straightforward but lengthy and tedious if one expands both sides of Eq. (13)

and performs a term-by-term comparison. For simplic-

ity, a more compact representation of Eqs. (14-29) can be expressed as

$$\begin{pmatrix} c_{\gamma_1-\gamma_3} s_{\delta_2} \\ c_{\gamma_1+\gamma_3} c_{\delta_2} \\ -s_{\gamma_1-\gamma_3} s_{\delta_2} \\ s_{\gamma_1+\gamma_3} c_{\delta_2} \end{pmatrix} \begin{pmatrix} c_{\delta_1-\delta_3} s_{\gamma_2} \\ c_{\delta_1+\delta_3} c_{\gamma_2} \\ -s_{\delta_1-\delta_3} s_{\gamma_2} \\ s_{\delta_1+\delta_3} c_{\gamma_2} \end{pmatrix}^T = \begin{pmatrix} c_{\gamma_5} s_{\delta_4+\delta_6} \\ c_{\gamma_5} c_{\delta_4+\delta_6} \\ s_{\gamma_5} s_{\delta_4-\delta_6} \\ s_{\gamma_5} c_{\delta_4-\delta_6} \end{pmatrix} \begin{pmatrix} s_{\gamma_4+\gamma_6} c_{\delta_5} \\ c_{\gamma_4+\gamma_6} c_{\delta_5} \\ s_{\gamma_4-\gamma_6} s_{\delta_5} \\ c_{\gamma_4-\gamma_6} s_{\delta_5} \end{pmatrix}^T, \quad (30)$$

Based on this theorem, we show explicitly in Table I the YBE analysis for six free-fermion Hamiltonians where the reflection, as the preprocessing step prior to the compression, is accomplished algebraically. Here, the Hamiltonian operator \hat{H} takes at most two terms from the set $\{H_X, H_Y, H_Z\}$, where

$$H_X = - \sum_{j=1}^{n-1} J_x \sigma_j^x \sigma_{j+1}^x, \quad (31)$$

$$H_Y = - \sum_{j=1}^{n-1} J_y \sigma_j^y \sigma_{j+1}^y, \quad (32)$$

$$H_Z = - \sum_{j=1}^{n-1} J_z \sigma_j^z \sigma_{j+1}^z. \quad (33)$$

In practice, the algebraic relations between rotations and phases can be further simplified since we care about only one solution (not all the solutions) that satisfies these algebraic relations. For example, for $\hat{H} = H_X$, an apparent solution is to let $\gamma_6 = 0$ (such that $\gamma_4 = \gamma_2$) and $\gamma_5 = \gamma_1 + \gamma_3$. Also, for $\hat{H} = H_X + H_Z$, if we do not consider the edge cases (that lead to singularities in the sine and cosine functions), (γ_i, δ_i) ($i = 4, 5, 6$) can be obtained from the following simplified trigonometric relations:

$$\tan([\gamma_4 + \gamma_6]/2) = \tan(\gamma_2/2) \frac{\cos([\delta_1 - \delta_3]/2)}{\cos([\delta_1 + \delta_3]/2)}, \quad (34)$$

$$\tan([\gamma_4 - \gamma_6]/2) = -\tan(\gamma_2/2) \frac{\sin([\delta_1 - \delta_3]/2)}{\sin([\delta_1 + \delta_3]/2)}, \quad (35)$$

$$\tan([\delta_4 + \delta_6]/2) = \tan(\delta_2/2) \frac{\cos([\gamma_1 - \gamma_3]/2)}{\cos([\gamma_1 + \gamma_3]/2)}, \quad (36)$$

$$\tan([\delta_4 - \delta_6]/2) = \tan(\delta_2/2) \frac{\sin([\gamma_1 - \gamma_3]/2)}{\sin([\gamma_1 + \gamma_3]/2)}, \quad (37)$$

$$\tan(\gamma_5/2) = \tan([\gamma_1 + \gamma_3]/2) \frac{\cos([\delta_4 + \delta_6]/2)}{\cos([\delta_4 - \delta_6]/2)}, \quad (38)$$

$$\tan(\delta_5/2) = -\tan([\delta_1 + \delta_3]/2) \frac{\cos([\gamma_4 + \gamma_6]/2)}{\cos([\gamma_4 - \gamma_6]/2)}. \quad (39)$$

V. TIME DYNAMICS ON A QUANTUM DEVICE

As a proof of concept and to highlight the impact of compressed circuits on a real noisy quantum device (IBM-Manila, average CNOT error $\sim 10^{-3}$, average read-out error $\sim 10^{-2}$ and 8192 shots), we performed a time dynamics simulation of the XY Hamiltonian with three spins. We computed the time-dependent staggered magnetization, $m_s(t)$, which can be connected to the antiferromagnetism and ferrimagnetism in materials as follows:

$$m_s(t) = \frac{1}{N} \sum_i (-1)^i \langle \sigma_z(t) \rangle. \quad (40)$$

The initial state is the ground state (Neél state) of the XY Hamiltonian, defined as $\Psi_0 = |\uparrow\downarrow\uparrow\downarrow \dots \uparrow\downarrow\rangle$. The staggered magnetization of the Neél state is one. We performed the time evolution for 2.5 units of time with a Trotter step size of 0.025 units.

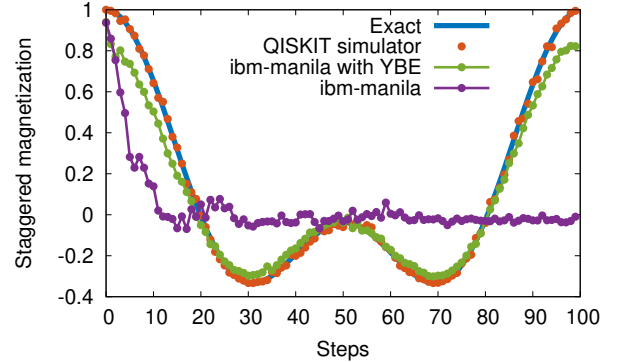


FIG. 5. Comparison of time dynamics for 3 spins with the XY ($J_x = -0.8$ and $J_y = -0.2$) Heisenberg Hamiltonian on the IBM (Manila) device (8,192 shots) with and without compression. Results from the Qiskit simulator serve as a baseline. Note that for simulating the XY model, each two-qubit gate includes two CNOTs, therefore the compressed circuit for the simulation only includes six CNOTs constituting three layers in comparison with 400 CNOTs without compression.

Figure 5 shows the evolution of the staggered magnetization for three spins with parameters $J_x = -0.8$ and $J_y = -0.2$. We choose different parameters for J_x and J_y

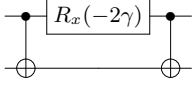
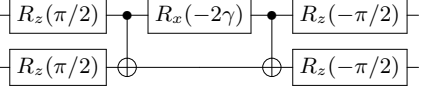
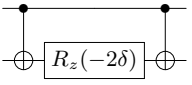
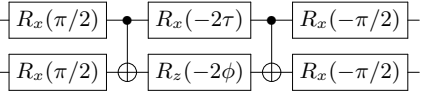
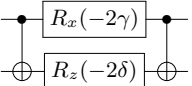
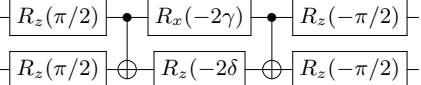
| Hamiltonian | Time Propagator | Time Propagator Circuit | Necessary Conditions for YBE |
|-------------|--|--|--|
| H_X | $e^{-itH_X/\hbar} = \mathcal{R}(\gamma, \delta = 0)$ |  | $s_{\gamma_2} c_{\gamma_1+\gamma_3} = c_{\gamma_5} s_{\gamma_4+\gamma_6}$, $c_{\gamma_2} c_{\gamma_1+\gamma_3} = c_{\gamma_5} c_{\gamma_4+\gamma_6}$ $s_{\gamma_2} s_{\gamma_1+\gamma_3} = s_{\gamma_5} s_{\gamma_4+\gamma_6}$, $c_{\gamma_2} s_{\gamma_1+\gamma_3} = s_{\gamma_5} c_{\gamma_4+\gamma_6}$ |
| H_Y | $e^{-itH_Y/\hbar} = U_1 \mathcal{R}(\gamma, \delta = 0) U_1^\dagger$ |  | Same as above |
| H_Z | $e^{-itH_Z/\hbar} = \mathcal{R}(\gamma = 0, \delta)$ |  | $c_{\delta_1+\delta_3} s_{\delta_2} = s_{\delta_4+\delta_6} c_{\delta_5}$, $s_{\delta_1+\delta_3} c_{\delta_2} = c_{\delta_4+\delta_6} s_{\delta_5}$ $c_{\delta_1+\delta_3} c_{\delta_2} = c_{\delta_4+\delta_6} c_{\delta_5}$, $s_{\delta_1+\delta_3} s_{\delta_2} = s_{\delta_4+\delta_6} s_{\delta_5}$ |
| $H_X + H_Y$ | $e^{-it(H_X+H_Y)/\hbar} = U_2 \mathcal{R}(\tau, \phi) U_2^\dagger$ $\tau = \gamma + \delta, \phi = \gamma - \delta$ |  | (τ, ϕ) -relation is analogous to Eqs. (14-29) |
| $H_X + H_Z$ | $e^{-it(H_X+H_Z)/\hbar} = \mathcal{R}(\gamma, \delta)$ |  | Eqs. (14-29) |
| $H_Y + H_Z$ | $e^{-it(H_Y+H_Z)/\hbar} = U_1 \mathcal{R}(\gamma, \delta) U_1^\dagger$ |  | Eqs. (14-29) |

TABLE I. YBE analysis for six free-fermion Hamiltonians. $U_1 = R_z(\pi/2) \otimes R_z(\pi/2)$ and $U_2 = R_x(\pi/2) \otimes R_x(\pi/2)$. The possible extension to Heisenberg model Hamiltonians with a transverse field is briefly discussed in Appendix B

to make the system anisotropic. The first component in Fig. 5 is the exact evolution of staggered magnetization for the XY model, which serves as a reference. The second component is a simulation using the Qiskit simulator with no noise, which provides the estimation for running this evolution on a noise-free quantum computer. The third component is the simulation result from the compressed circuit, which captures the dynamics for almost every time step. The compressed circuits are produced by repeated use of the YBE and merge identity. In contrast, results from a run on the same device with IBM-compiled circuits deviate quickly after the third time step. This comparison shows the impact of compressed circuits on a noisy quantum computer.

The compressed circuit simulation on a noisy quantum device shows an exceptional match with the exact evolution of staggered magnetization between steps 20 and 80. Also, the staggered magnetizations at the initial (i 20 steps) and the last (i 80 steps) phases are similar in magnitude. Nevertheless, the amount of quantum error and its type are different in the two observations. At the zeroth step, the error mainly comes from state preparation. At the last step, however, other errors from state evolution enter and make large deviations from the exact staggered magnetization on top of the state preparation error. Depolarization noise converts a pure state to a maximally mixed state. Staggered magnetization for the maximally mixed state is zero. It is evident for uncompressed circuits, where staggered magnetization after the tenth step reaches zero and stays there for later steps. Therefore,

depolarization noise favors states that have a staggered magnetization of zero. It is also the main contributor to the unparalleled overlap of simulation results from compressed circuits and exact evolution. The compressed circuits will overlap more with exact evolution, irrespective of J_x and J_y , because of small depth. The results obtained from compressed circuits have controllable errors due to Trotter decomposition. The absolute error can be reduced with a smaller step size. However, a small step size increases the number of alternative layers, which can be compressed by using our scheme to make it polynomial depth again. Therefore, our scheme is implicitly an error mitigation technique, which allows for significantly reducing quantum circuit depth, and (together with other error mitigation techniques) for systematic convergence to the exact answer without increasing the circuit size. The only bottleneck is preprocessing of the circuit on a classical computer (see Appendix A for detailed analysis). Performing the YBE combined with the merge identity is computationally straightforward because of analytical expressions that we have derived. We note, however, that multiple time usages of both can make the compression scheme computationally expensive for a large number of qubits. Computational complexity analysis for our compression scheme is currently being pursued and will be the subject of a future paper.

VI. CONCLUSIONS AND OUTLOOK

We have shown how the YBE can be utilized to compress and produce a shallow quantum circuit for efficient time dynamics simulations of 1D lattice spin chains with nearest-neighbor interactions on real quantum computers. The depth of quantum circuits for each time step is independent of time and step size and depends only on the number of spins. In particular, the depth of the compressed circuit is rigorously a linear function of the system size for the studied Heisenberg model Hamiltonians, and the number of CNOT gates in the compressed circuit only scales quadratically with system size. This allows for simulations of time dynamics of very large 1D spin chains. Moreover, we derived the compressed circuit representations for different special cases of the Heisenberg Hamiltonian. To demonstrate the efficacy of the developed technique, we performed a time dynamics simulation of three spins on an IBM quantum computer and compared both compressed and uncompressed quantum circuits. The results for the first time confirmed the superiority of the YBE formulation to perform dynamics for a large number of steps, and connected our work to the broader and deeper context of the YBE duality and integrable quantum computation.

A promising application of this technique is to explore the compression of any circuit as part of the circuit compilation step. The general nature of the technique suggests that it could work for any circuit containing repeating gate motifs. It could be used, for example, to compress certain types of graph instances to solve combinatorial optimization problems using QAOA [73]. In particular, certain ZZ gate (a combination of $CNOT$, R_z , and $CNOT$ gates) motifs could be compressed. Another aspect of YBE compression scheme is the control of Trotter error. Smaller step size result in smaller trotter error, which result in large number of trotter steps. This compression scheme allows to compress to a constant number of trotter steps, which only depends on system size. It is very much evident in Fig. 5, where for any time and any step size it only requires three trotter step for time evolution of 3-spin system.

We have noticed some other techniques developed for the quantum simulation of the time evolution of model Hamiltonian reporting similar performance. For example, in the post-quench dynamics simulations of the Lieb-Schultz-Mattis model using an adaptive variational approach [74], a quadratic scaling of the number of CNOTs with number of qubits is observed. Similar performance has also been reported where the disentanglement of the 1D XY model Hamiltonian is achieved by resorting to Fourier and Bogoliubov transformations [40], and the depth of the circuit grows as $\mathcal{O}(N \log N)$.

Finally, it is worth pointing out that in this paper we are still dealing with the integrable models, for which classical approaches such as the time-dependent density matrix renormalization group (t -DMRG) [75–77] has shown to be time efficient (i.e. the computation time

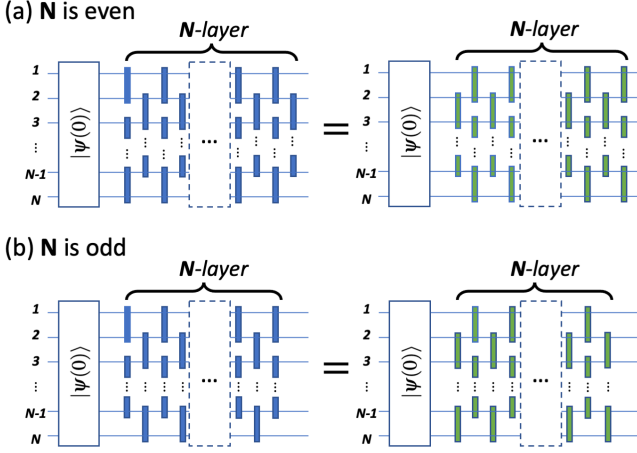
and memory scale as polynomial functions of physical time in the thermodynamic limit). Specifically, studies by Prosen and Žnidarič have shown that the scaling of the classical computation resources for simulations of quantum 1D lattices with local interactions is closely connected to the integrability of the Hamiltonian. [77] Therefore, it does not make sense to discuss the quantum advantage (i.e., a substantial computational advantage of quantum computing over classical computing) at the present stage. However, our work provides a path for efficient simulations of certain classes of integrable Hamiltonians, which is a stepping stone for demonstrating quantum advantage on NISQ devices where quantum dynamics of more complex (non-integrable) quantum systems has been proposed as a prime candidate. The reason why it has not been achieved yet is that NISQ devices are currently only able to simulate circuits reliably on shallow depth circuits. The YBE technique presented in this work is a potential direction to solve this problem, thus bringing the ability to solve practical problems one step closer on quantum computers.

ACKNOWLEDGMENT

This material is based upon work supported by the U.S. Department of Energy, Office of Science, National Quantum Information Science Research Centers. Y.A. acknowledges support from the U.S. Department of Energy, Office of Science, under contract DE-AC02-06CH11357 at Argonne National Laboratory. S.G thanks Prof. James Daniel Whitfield for insightful discussions.

Appendix A: The proof of vertical/horizontal reflection symmetry in the quantum circuit employed for simulating the time evolution of 1D Heisenberg model with Hamiltonian defined in Table. I

In the main text, we have demonstrated a vertical reflection symmetry, i.e. the three-site YBE relation, exists for three-layer in the circuit structure used for simulating the time evolution of the three-spin Heisenberg model with Hamiltonian defined in Tab. I. In addition, we have demonstrated that a horizontal reflection symmetry relation, derived from the three-spin YBE relation, exists for the four-layer circuit structure used for simulating the time evolution of the four spin Heisenberg model. Here, we show that a vertical or horizontal reflection symmetry exists for the N -layer ($N \geq 3$ can be an arbitrarily large integer) in the similar circuit structure used for simulating the time evolution of Heisenberg model Hamiltonian defined in Table. I governing the N -spin system. Explicitly, as shown in Fig. 6, when N is even, a horizontal reflection exists, and when N is odd, a vertical reflection exists.



The proof for the existence of a reflection relation can be shown by induction where for 3- and 4-spin systems the vertical and horizontal reflections are already known and shown in the main text. If we assume for the $(N-1)$ -spin system that a reflection (either vertical or horizontal) exists for every $(N-1)$ -layer in its time evolution circuit, we then only need to prove that a reflection relation also exists for every N -layer in the time evolution circuit for the N -spin system. To see that, we can transform the corresponding circuit structure in three steps, which are showed diagrammatically in Fig. 7 and interpreted as follows.

- Step 1. As shown in Fig. 7a, in this step the two-qubit gates in the top row can be consecutively moved (as seen from the orange arrow) to the right and tucked between the two-qubit gates in the last layer. From the r.h.s of Fig. 7a, this step can physically be viewed as “downfolding” the propagation of the N -qubit system over $N\Delta t$ time into the propagation of the $(N-1)$ -qubit system over $(N-1)\Delta t$ multiplied by the propagation of the N -qubit system over one time step Δt .
- Step 2. As shown in Fig. 7b, since we have assumed the existence of the reflection symmetry in the time evolution circuit for $(N-1)$ -spin system, this reflection can then be directly applied to obtain the r.h.s of Fig. 7b.
- Step 3. As shown in Fig. 7c, finally by performing consecutive three-spin YBE backwards we can move the two-qubit gates in the original last layer (denoted by the blue blocks) back to the top row, and the resulting circuit structure exhibits a re-

flected circuit structure compared with the original circuit (i.e. l.h.s of Fig. 7a).

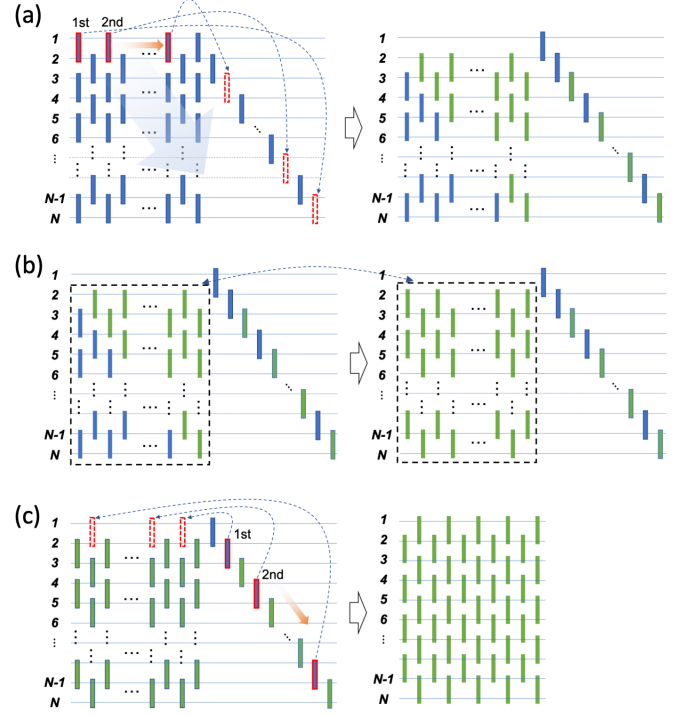


FIG. 7. A diagrammatic proof of the reflection symmetry in the quantum circuit employed for simulating the time evolution of 1D Heisenberg model with Hamiltonian defined in Table. I. Here, the blue blocks denote the original two-qubit gates, the green blocks denote the two-qubit gates after YBE transformation, and the red dashed blocks denote the destinations that are connected by dashed arrow curves to the highlighted blue blocks after performing consecutive three-spin YBE transformations. The orange arrow indicates the direction for moving the two-qubit gates in each step.

Remarkably, in the above proof we have utilized the three-site YBE transformations consecutively in Steps 1 and 3. The consecutive three-site YBE transformation can be viewed as a “long distance” YBE. To see how it works, take a 10-qubit time evolution circuit as an example, as can be seen from Fig. 8, eight consecutive three-site YBE operations can be performed in order to move a top left two-qubit gate to a bottom right position. In general, we can see for a two-qubit gate being moved from qubits i and $i+1$ to qubits j and $j+1$ ($j \neq i$) through the diagonal direction, a total of $\|j-i\|$ consecutive three-site YBE operations would be needed.

Regarding the scaling of the reflection operation for the N -layer time evolution circuit of an N -qubit system, there are $N-1$ two-qubit gates need to be moved back and forth between the side layer and the top layer in Steps 1 and 3, which contributes to $\frac{N(N-1)}{2}$ three-site YBE operations. Since Step 2 indicates a recursion, the total number of three-site YBE operations in all three

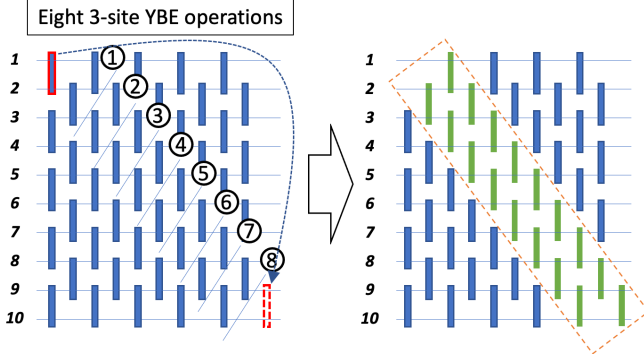


FIG. 8. In the time evolution circuit of a 10-qubit Heisenberg model, the top left two-qubit (blue block highlighted by red frame) gate can be gradually moved downward to the bottom right position (denoted by the dashed red block) through eight consecutive three-site YBE operations (labelled by circled numbers). As a result of the eight consecutive three-site YBE operations, all the two-qubit gates in the diagonal direction (included in the red dashed frame on the r.h.s.) need to update their rotations and phase factors.

steps scales as

$$\mathcal{O}(N^2) + \mathcal{O}((N-1)^2) + \dots = \mathcal{O}(N^3). \quad (\text{A1})$$

It is worth mentioning that the actual time for executing the reflection operation can be reduced by exploiting the parallel operations (i.e. simultaneously performing multiple three-site YBE reflection operations), or by directly figuring out the algebraic relations corresponding to the consecutive three-site YBE operations over a large number of qubit sites to bypass the intermediate operations.

Appendix B: Extension to simulating the time evolution of 1D Heisenberg model with a transverse field

It is possible to employ our YBE circuit compression technique for some model Hamiltonians with a transverse field. Take XX+Z model as an example, since the XX+Z model Hamiltonian can be written as

$$H = H_{XX} + H_Z \quad (\text{B1})$$

with

$$H_{XX} = J_x \sum_i (\sigma_i^x \sigma_{i+1}^x + \sigma_i^y \sigma_{i+1}^y),$$

$$H_Z = h_z \sum_i \sigma_i^z,$$

$$[H_{XX}, H_Z] = 0,$$

there will be no Trotter error in the following decomposition

$$e^{-iHt} = e^{-iH_{XX}t} e^{-iH_Zt} = e^{-iH_Zt} e^{-iH_{XX}t}, \quad (\text{B2})$$

from which we can see

$$[e^{-iH_{XX}t}, e^{-iH_Zt}] = 0. \quad (\text{B3})$$

Therefore, as shown in Fig. 9 the time evolution circuit for the XX+Z model can be equivalently transformed through consecutive swaps between blue and green gate layers to a circuit for pure XX model plus a single Rz layer. We notice that a similar “turn over” transforma-

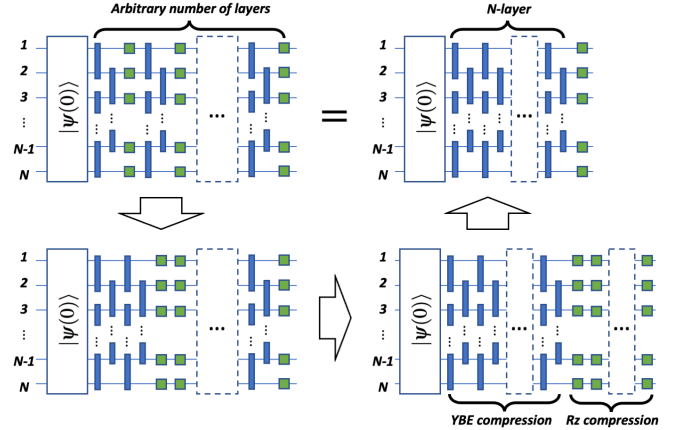


FIG. 9. Circuit compression for XX+Z model. Two-qubit gates for XX interaction are denoted by blue blocks, and single qubit Rz gates are denoted by green blocks. Note that blue and green blocks commute.

tion for model Hamiltonians with a transverse field has been reported in Ref. [47], while the YBE transformation for other models with a transverse field are currently under exploration.

- J. Kim, S. Kimmel, M. Lange, S. Lloyd, M. D. Lukin, D. Maslov, P. Maunz, C. Monroe, J. Preskill, M. Roetteler, M. J. Savage, and J. Thompson, Quantum computer systems for scientific discovery, *PRX Quantum* **2**, 10.1103/prxquantum.2.017001 (2021).
- [2] M. Suzuki, Relationship between d-dimensional quantum spin systems and (d+1)-dimensional Ising systems: Equivalence, critical exponents and systematic approximations of the partition function and spin correlations, *Progress of Theoretical Physics* **56**, 1454 (1976).
- [3] S. Sachdev, *Quantum phase transitions* (Cambridge University Press, 2011).
- [4] R. Shankar, *Quantum Field Theory and Condensed Matter: An Introduction* (Cambridge University Press, 2017).
- [5] B. Sutherland, *Beautiful models: 70 years of exactly solved quantum many-body problems* (World Scientific, 2004).
- [6] P. Benioff, The computer as a physical system: A microscopic quantum mechanical Hamiltonian model of computers as represented by Turing machines, *Journal of Statistical Physics* **22**, 563 (1980).
- [7] R. P. Feynman, Simulating physics with computers, *Int. J. Theor. Phys* **21** (1982).
- [8] National QIS Research Centers, U.S. DOE Office of Science(SC), <https://science.osti.gov/Initiatives/QIS/QIS-Centers> (2021), [Online; accessed November, 17 2021].
- [9] J. Preskill, Quantum computing in the NISQ era and beyond, *Quantum* **2**, 79 (2018).
- [10] M. Jimbo, Introduction to the Yang–Baxter equation, *International Journal of Modern Physics A* **4**, 3759 (1989).
- [11] H. Bethe, Zur theorie der metalle, *Z. Physik* **71**, 205 (1931).
- [12] M. T. Batchelor, The bethe ansatz after 75 years, *Physics Today* **60**, 36 (2007).
- [13] C.-N. Yang, Some exact results for the many-body problem in one dimension with repulsive delta-function interaction, *Physical Review Letters* **19**, 1312 (1967).
- [14] R. J. Baxter, *Exactly solved models in statistical mechanics* (Elsevier, 2016).
- [15] J. Perk and H. Au-Yang, *Encyclopedia of Mathematical Physics* (2006).
- [16] W. Heisenberg, Zur theorie des ferromagnetismus, *Z. Physik* **49**, 619 (1928).
- [17] M. Takahashi, One-Dimensional Heisenberg Model at Finite Temperature, *Progress of Theoretical Physics* **46**, 401 (1971).
- [18] M. Karbach, G. Müller, H. Gould, and J. Tobochnik, Introduction to the Bethe ansatz I, *Computers in Physics* **11**, 36 (1997).
- [19] M. Karbach, K. Hu, and G. Müller, Introduction to the Bethe ansatz II, *Computers in Physics* **12**, 565 (1998).
- [20] M. Karbach, K. Hu, and G. Müller, Introduction to the Bethe ansatz III (2000), arXiv:0008018 [cond-mat.stat-mech].
- [21] L. D. Faddeev, How algebraic Bethe ansatz works for integrable model (1996), arXiv:9605187 [hep-th].
- [22] E. H. Lieb and W. Liniger, Exact analysis of an interacting Bose gas. I. the general solution and the ground state, *Phys. Rev.* **130**, 1605 (1963).
- [23] E. H. Lieb, Exact analysis of an interacting Bose gas. II. the excitation spectrum, *Phys. Rev.* **130**, 1616 (1963).
- [24] F. Essler, H. Frahm, F. Göhmann, A. Klümper, and V. Korepin, *The One-Dimensional Hubbard Model* (Cambridge University Press, 2005).
- [25] F. Calogero, Ground state of a onedimensional Nbody system, *Journal of Mathematical Physics* **10**, 2197 (1969).
- [26] F. Calogero, Solution of a threebody problem in one dimension, *Journal of Mathematical Physics* **10**, 2191 (1969).
- [27] F. Calogero, Solution of the onedimensional Nbody problems with quadratic and/or inversely quadratic pair potentials, *Journal of Mathematical Physics* **12**, 419 (1971).
- [28] B. Sutherland, Quantum manybody problem in one dimension: Ground state, *Journal of Mathematical Physics* **12**, 246 (1971).
- [29] B. Sutherland, Quantum manybody problem in one dimension: Thermodynamics, *Journal of Mathematical Physics* **12**, 251 (1971).
- [30] J. D. Johnson, S. Krinsky, and B. M. McCoy, Vertical-arrow correlation length in the eight-vertex model and the low-lying excitations of the $X - Y - Z$ Hamiltonian, *Phys. Rev. A* **8**, 2526 (1973).
- [31] A. Luther, Eigenvalue spectrum of interacting massive fermions in one dimension, *Phys. Rev. B* **14**, 2153 (1976).
- [32] R. Orbach, Linear antiferromagnetic chain with anisotropic coupling, *Phys. Rev.* **112**, 309 (1958).
- [33] M. Rigol, V. Dunjko, V. Yurovsky, and M. Olshanii, Relaxation in a completely integrable many-body quantum system: An ab initio study of the dynamics of the highly excited states of 1D lattice hard-core bosons, *Phys. Rev. Lett.* **98**, 050405 (2007).
- [34] A. C. Cassidy, C. W. Clark, and M. Rigol, Generalized thermalization in an integrable lattice system, *Phys. Rev. Lett.* **106**, 140405 (2011).
- [35] J.-S. Caux and F. H. L. Essler, Time evolution of local observables after quenching to an integrable model, *Phys. Rev. Lett.* **110**, 257203 (2013).
- [36] M. Fagotti, Dynamical phase transitions as properties of the stationary state: Analytic results after quantum quenches in the spin-1/2 XXZ chain (2013), arXiv:1308.0277 [cond-mat.stat-mech].
- [37] B. Pozsgay, The generalized Gibbs ensemble for Heisenberg spin chains, *J. Stat. Mech.* **2013**, P07003 (2013).
- [38] N. A. Sinitsyn and F. Li, Solvable multistate model of landau-zener transitions in cavity QED, *Physical Review A* **93**, 063859 (2016).
- [39] N. A. Sinitsyn, E. A. Yuzbashyan, V. Y. Chernyak, A. Patra, and C. Sun, Integrable time-dependent quantum Hamiltonians, *Physical Review Letters* **120**, 190402 (2018).
- [40] F. Verstraete, J. I. Cirac, and J. I. Latorre, Quantum circuits for strongly correlated quantum systems, *Phys. Rev. A* **79**, 032316 (2009).
- [41] S.-H. Lin, R. Dilip, A. G. Green, A. Smith, and F. Pollmann, Real-and imaginary-time evolution with compressed quantum circuits, *PRX Quantum* **2**, 010342 (2021).
- [42] C. Cirstoiu, Z. Holmes, J. Iosue, L. Cincio, P. J. Coles, and A. Sornborger, Variational fast forwarding for quantum simulation beyond the coherence time, *npj Quantum Information* **6**, 1 (2020).
- [43] Y. Atia and D. Aharonov, Fast-forwarding of hamiltonians and exponentially precise measurements, *Nature Communications* **8**, 1 (2017).
- [44] N. F. Berthussen, T. V. Trevisan, T. Iadecola, and P. P.

- Orth, Quantum dynamics simulations beyond the coherence time on noisy intermediate-scale quantum hardware by variational trotter compression, *Physical Review Research* **4**, 023097 (2022).
- [45] F. Barratt, J. Dborin, M. Bal, V. Stojevic, F. Pollmann, and A. G. Green, Parallel quantum simulation of large systems on small nisc computers, *npj Quantum Information* **7**, 1 (2021).
- [46] L. Bassman, R. V. Beeumen, E. Younis, E. Smith, C. Iancu, and W. A. de Jong, Constant-depth circuits for dynamic simulations of materials on quantum computers (2021), arXiv:2103.07429 [quant-ph].
- [47] E. Kkc, D. Camps, L. Bassman, J. K. Freericks, W. A. de Jong, R. V. Beeumen, and A. F. Kemper, Algebraic compression of quantum circuits for Hamiltonian evolution, *Physical Review A* **105**, 10.1103/physreva.105.032420 (2022).
- [48] D. Camps, E. Kkc, L. Bassman, W. A. de Jong, A. F. Kemper, and R. Van Beeumen, An algebraic quantum circuit compression algorithm for hamiltonian simulation (2021).
- [49] P. Fazekas, *Lecture notes on electron correlation and magnetism*, Vol. 5 (World scientific, 1999).
- [50] R. Skomski, *Simple models of magnetism* (Oxford University Press, 2008).
- [51] A. S. T. Pires, *Theoretical Tools for Spin Models in Magnetic Systems* (IOP Publishing, 2021).
- [52] I. de PR Moreira and F. Illas, A unified view of the theoretical description of magnetic coupling in molecular chemistry and solid state physics, *Physical Chemistry Chemical Physics* **8**, 1645 (2006).
- [53] G. David, N. Guihéry, and N. Ferré, What are the physical contents of hubbard and heisenberg hamiltonian interactions extracted from broken symmetry dft calculations in magnetic compounds, *Journal of Chemical Theory and Computation* **13**, 6253 (2017).
- [54] E. Lieb, T. Schultz, and D. Mattis, Two soluble models of an antiferromagnetic chain, *Ann. Phys.* **16**, 407 (1961).
- [55] S. Katsura, Statistical mechanics of the anisotropic linear Heisenberg model, *Phys. Rev.* **127**, 1508 (1962).
- [56] S. Katsura, Statistical mechanics of the anisotropic linear Heisenberg model, *Phys. Rev.* **129**, 2835 (1963).
- [57] T. Niemeijer, Some exact calculations on a chain of spins 12, *Physica* **36**, 377 (1967).
- [58] R. Kosloff, Time-dependent quantum-mechanical methods for molecular dynamics, *The Journal of Physical Chemistry* **92**, 2087 (1988).
- [59] D. J. Tannor, *Introduction to quantum mechanics: a time-dependent perspective* (University Science Books, Sausalito, CA, 2007).
- [60] Y. Nam and D. Maslov, Low-cost quantum circuits for classically intractable instances of the hamiltonian dynamics simulation problem., *npj Quantum Inf.* **5**, 44 (2019).
- [61] A. M. Childs, D. Maslov, Y. Nam, N. J. Ross, and Y. Su, Toward the first quantum simulation with quantum speedup, *Proc. Natl. Acad. Sci. U.S.A.* **115**, 9456 (2018), <https://www.pnas.org/doi/pdf/10.1073/pnas.1801723115>.
- [62] S. Raesi, N. Wiebe, and B. C. Sanders, Quantum-circuit design for efficient simulations of many-body quantum dynamics, *New J. Phys.* **14**, 103017 (2012).
- [63] M. Reiher, N. Wiebe, K. M. Svore, D. Wecker, and M. Troyer, Elucidating reaction mechanisms on quantum computers, *Proc. Natl. Acad. Sci. U.S.A.* **114**, 7555 (2017).
- [64] R. Babbush, J. McClean, D. Wecker, A. Aspuru-Guzik, and N. Wiebe, Chemical basis of trotter-suzuki errors in quantum chemistry simulation, *Phys. Rev. A* **91**, 022311 (2015).
- [65] R. J. Baxter, Partition function of the eight-vertex lattice model, *Annals of Physics* **70**, 193 (1972).
- [66] M.-L. Ge, K. Xue, R.-Y. Zhang, and Q. Zhao, Yang-Baxter equations and quantum entanglements, *Quantum Information Processing* **15**, 5211 (2016).
- [67] C. Nayak, S. H. Simon, A. Stern, M. Freedman, and S. Das Sarma, Non-Abelian anyons and topological quantum computation, *Rev. Mod. Phys.* **80**, 1083 (2008).
- [68] L. H. Kauffman and S. J. J. Lomonaco, Topological quantum information theory, in *Proceedings of Symposia in Applied Mathematics*, Vol. 68, edited by S. J. Lomonaco (AMS, Washington, DC, 2010).
- [69] Y. Zhang, Integrable quantum computation, *Quantum Inf. Process.* **12**, 631 (2013).
- [70] F. A. Vind, A. Foerster, I. S. Oliveira, R. S. Sarthour, D. d. O. Soares-Pinto, A. M. d. Souza, and I. Roditi, Experimental realization of the Yang-Baxter equation via NMR interferometry, *Scientific reports* **6**, 1 (2016).
- [71] M. T. Batchelor and A. Foerster, Yang-Baxter integrable models in experiments: from condensed matter to ultracold atoms, *Journal of Physics A: Mathematical and Theoretical* **49**, 173001 (2016).
- [72] R. S. Chen, Generalized yang-baxter equations and braiding quantum gates, *J. Knot Theory Ramif.* **21**, 1250087 (2012).
- [73] E. Farhi, J. Goldstone, and S. Gutmann, A quantum approximate optimization algorithm (2014), arXiv:1411.4028 [quant-ph].
- [74] Y.-X. Yao, N. Gomes, F. Zhang, C.-Z. Wang, K.-M. Ho, T. Iadecola, and P. P. Orth, Adaptive variational quantum dynamics simulations, *PRX Quantum* **2**, 030307 (2021).
- [75] D. Gobert, C. Kollath, U. Schollwöck, and G. Schütz, Real-time dynamics in spin- $\frac{1}{2}$ chains with adaptive time-dependent density matrix renormalization group, *Phys. Rev. E* **71**, 036102 (2005).
- [76] T. J. Osborne, Efficient approximation of the dynamics of one-dimensional quantum spin systems, *Phys. Rev. Lett.* **97**, 157202 (2006).
- [77] T. Prosen and M. Žnidarič, Is the efficiency of classical simulations of quantum dynamics related to integrability?, *Physical Review E* **75**, 015202 (2007).